# The Effect of $Al_2O_3$ Addition on Solidification Process of Phase Change Material: A Case Study on Heating of Automobile Cabin in Cold Climate Conditions

Habib Gürbüz[1*], Himmet Emre Aytaç[2], Hüseyin Cahit Hamamcioğlu[2] and Hüsameddin Akçay[1]

0000-0001-5157-6227, 0000-0002-8320-5380, 0000-0001-5009-2001, 0000-0002-5704-670X

[1] *Department of Automotive Engineering, Faculty of Engineering, Süleyman Demirel University, 32200, Isparta/Turkey*
[2] *Graduate School of Natural and Applied Sciences, Süleyman Demirel University, 3200, Isparta/Turkey*

## Abstract

In this paper, an experimental investigation is revealed on the solidification process of the latent heat thermal energy storage (LHTES) system, in which the heat energy emitted into the atmosphere with the exhaust gases of ICE vehicles is stored by phase change material (PCM) enhanced with nanoparticles ($Al_2O_3$). In the study using RT55 paraffin wax as the PCM, the interior heating process of a typical sedan automobile in cold climate conditions is used as the heat release medium for the LHTES system. Experimental studies carried out in real climatic conditions were repeated for pure paraffin (RT55) and five different $Al_2O_3$ fractions (5 wt.%, 10 wt.%, 15 wt.%, 20 wt.%, and 25 wt.%). Experiments are performed in an optical PCM container and are completed after 1200 seconds (20 minutes). The heat energy stored in the PCM container is discharged to the automobile cabin via the closed-circuit liquid circulation system by the heating radiator system in the automobile cabin. The findings showed that the solidification process is improved considerably up to 10 wt.% $Al_2O_3$ fractions compared with pure paraffin RT55, and the temperature in the cabin could be increased by approximately 29%. In addition, the $Al_2O_3$ fraction increased by more than 10 wt.%, which has a negative effect on the improvement in the solidification process, but higher solidification ability and in-cabinet temperature were obtained with all $Al_2O_3$ fractions compared to pure RT55.

*Keywords*: Exhaust waste heat recovery, LHTES, PCM, Nanoparticles addition, Heat discharge (Solidification), Automobile cabin interior heating.

## 1. Introduction

Recently, studies have drawn attention to the efficient use of existing energy resources to reduce the rate of fossil-based fuel consumption and atmospheric pollution [1]. All over the world, internal combustion engines (ICEs) have a large share in the consumption of existing energy resources. Therefore, it is of great importance to exhaust waste heat recovery in ICEs in order to ensure maximum efficiency from the fuels used. Only 30-40% of the total fuel energy of the ICE can be converted to useful work at the crankshaft. The remaining heat is discharged from the system via exhaust gases and engine cooling systems [2]. The reuse of waste heat energy lost by exhaust gases is of great importance in terms of reducing fuel consumption and emissions to the atmosphere [3]. In the literature, there are many studies used to meet the needs of vehicles or ICEs (i.e., vehicle cabin, catalytic converter and other equipment) in cold operating conditions by storing exhaust waste heat energy in thermal energy storage (TES) systems [4,5]. In TES

systems, it is possible to store waste heat energy by using phase change materials (PCMs) with a high latent heat enthalpy and to reuse the stored heat energy by again phase-changing when necessary [6]. With TES systems, the energy under conditions such as temperature, location, and power of the system can be stored for later use. The main purpose is to recover the lost energy during the production and use of energy. TES systems are a complete energy storage cycle that includes the processes of charging, storing, and discharging heat energy for later use [7]. Energy can be added to increase the temperature of a material. The energy related to temperature rise is called "sensible heat", and its formation depends on the temperature change and the specific heat of the material. Forming sensible heat can be discharged to another and/or cooler material or environment by heat transfer mechanisms (i.e., conduction, convection, or radiation). This method is widely used for the storage of energy in the form of heat and its reuse when necessary [8]. LHTES is the most efficient method of storing waste heat energy.

LHTES systems are energy storage structures in which materials that absorb or release heat are used from solid to solid, solid to liquid, liquid to gas or vice versa [9]. Currently, the most common type of transition marketed in bulk is solid/liquid PCMs. The solid-liquid PCMs are generally examined under the three main titles: organic, inorganic, and eutectic [10]. Each PCM has its own weak features. These weak points can be improved with some techniques and system design. Their long service life, environmental friendliness, and recycling potential make PCMs more attractive than other types of thermal energy storage systems [11]. Inorganic PCMs are composed of inorganic molecules. Inorganics provide a wider temperature range, higher volumetric energy storage capacities, and higher thermal conductivity values compared to organics [12]. The unstable working structure of these materials and their containers for long-term use remains a problem, limiting their use as a latent heat storage system [13]. Eutectic PCMs are materials that consist of more than one component and act as a single component in the melting and solidification processes. The main problem with these components is their high cost [14]. Common properties of organic phase transformation materials: Besides being stable and reliable, they do not cause corrosion of the system. This is because organic phase transformation materials typically contain a mixture of hydrocarbons such as long-chain paraffin and natural waxes. Organic phase transformation materials are classified with a wide range of melting temperatures rather than a single melting temperature value [15]. Paraffin wax is the most widely known and commercially used organic heat storage PCM. Many researchers state that paraffin is suitable due to its high heat of fusion, stable behavior, and thermal properties that do not deteriorate even after a large number of thermal cycles [16]. However, the low thermal conductivity of paraffin wax is its most important disadvantage. Nanoparticle additives with higher thermal conductivity [i.e., graphite (G), aluminium oxide ($Al_2O_3$), copper (Cu), copper oxide (CuO), gold (Au), silver (Ag), silicon carbide (SiC), titanium carbide (TiC), titanium oxide ($TiO_2$), and zinc oxide (ZnO)] are widely used to increase the thermal conductivity of PCM.

Dhinakaran et al. investigated the effect of adding $Al_2O_3$ nanoparticles to increase the thermal conductivity of PCM in a solar water heating system with PCM. The findings of the study showed that the thermal conductivity increased with the contribution of $Al_2O_3$ nanoparticles to the PCM, and as a result, the water temperature increased by 33% by providing more heat absorption [17]. Kumar et al. researched the effects of CuO and $Al_2O_3$ nanoparticles added to PCM in a low mass fraction (1.0 wt.%) on the thermal conductivity and thermal storage capabilities of PCM. As a result, it was determined that CuO and $Al_2O_3$ nanoparticle addition reduced the cooling effect of PCM by 40% and 31.42%, respectively. In addition, the addition of CuO and $Al_2O_3$ nanoparticles increased the thermal conductivity of PCM by 60.56% and 39.44%, respectively [18]. El-bahjaoui et al. examined the thermal performance of a solar LHTES system having an $Al_2O_3$ nanoparticle enhanced PCM and a flat plate solar collector. They determined that as the volume % of nanoparticles in PCM grew, so did the PCM's rate of melting. In addition, it is determined that 16.54 kJ of energy is stored in the PCM with a 40% storage efficiency [19]. Akib et al. investigated the thermal conductivity and phase change time for PCM consisting of paraffin wax added with nanoparticles. Carbon ions (Mul-tiwall carbon nanotubes_MWCNTs) and metallic ions ($Al_2O_3$) used as nanoparticles were added to paraffin wax at three different fractions such as 2 wt.%, 4 wt.%, and 6 wt.%. As a result, it was determined that the peak temperature of 65 °C was reached with the addition of $Al_2O_3$ nanoparticles, and the peak temperature was 6% higher than the other nanoparticles [20]. Haghighi et al. researched the effects of different nanoparticles such as CuO, $TiO_2$, $Al_2O_3$ and graphene added to PCM on the thermal properties of PCM. They found that PCM with 2 wt.% $TiO_2$ added has the maximum energy storage capacity (179.88 J/g), while PCM with 1 wt.% graphene added has the minimum energy storage capacity (120.38 J/g). In addition, while 3 wt.% graphene nanocomposites have the highest thermal conductivity coefficient, 1 wt.% $TiO_2$ nanocomposites have the lowest thermal conductivity [21]. Mehdi and Nosofor designed longitudinal fins with nanoparticles and developed a model for the variations in heat transfer in order to improve the energy recovery process in the triplex tube PCM system. Results show that fin-nanoparticle combinations revealed a stronger solidification effect than nanoparticles alone for the same volume utilization. In addition, increasing the fin volume exhibits higher performance when certain combinations are applied. The findings of the study showed that the time needed to complete solidification of the PCM can be decreased by 55% when using fins alone, 8% when using nanoparticles alone, and 30% when using a combination of fins and nanoparticles compared to the base model [22]. Wu et al. studied the melting and freezing properties of copper nanoparticle-added paraffin. As a result, the addition of nanoparticles significantly increased the heat transfer in the phase change process of PCMs. It was determined that the thermal conductivity increased by 14.2% in the solid state and 18.1% in the liquid state with 2% Cu added to PCM by weight. It was also observed that there is no linear relationship between the bulk concentration of Cu nanoparticles and the thermal conductivity of PCM [23]. Darzi et al. investigated the effect of fins use and nanoparticle (Cu) addition on the melting and solidification characteristics of PCM with a theoretical model. They noticed that the rate of melting and solidification increased with the addition of nanoparticles to the PCM. On the other hand, with the addition of 2 vol.% and 4 vol.% Cu nanoparticles, the total solidification time of PCM was reduced by 9% and 16%, respectively [24]. Motahar et al. researched the effect of $TiO_2$ nanoparticles dispersed in PCM on the solidification process. The findings showed that the $TiO_2$ nanoparticle dispersion increased the thermal conductivity of the PCM and, consequently, the solidified volume increased. It was observed that the solidification volume for 1 vol.%, 2 vol.%, and 4 vol.% $TiO_2$ nanoparticles fractions increased by 7%, 9%, and 18%, respectively [25]. On the other hand, the thermal properties of different paraffin waxes affect the melting and solidification processes of PCM. Gürbüz and Ateş used 3 different paraffin waxes (i.e., RT27, RT35, and RT55) to examine the optimum PCM for the LHTES system in which the exhaust waste heat energy of a single-cylinder, air coolant gasoline engine is stored. In the paper, they carried out experimental and numerical simulation studies, and they found a close correlation of 7.8% between experimental studies and numerical simulation results. In the numerical studies for the equal

storage volume, they were able to energy store 1879 kJ with a RT27 by 88.8% liquefaction fraction, 1556 kJ with a RT35 by 86% liquefaction fraction, and 1846 kJ with a RT55 by 83.9% liquefaction fraction. They also stated that the heat exchanger efficiency in which the PCM was stored was 11%, 9.4%, and 11.1% for RT27, RT35, and RT55, respectively [26].

Literature studies reveal the positive effect of the contribution of nanoparticles to PCM on the melting and solidification process. However, most of the studies have fixed facility system infrastructure. Studies on energy storage and reuse in nanocomposite PCMs for exhaust waste heat conversion of mobility systems such as internal combustion engine cars are very limited. In this paper, an experimental study was performed on the solidification process of the LHTES system, in which the heat energy emitted into the atmosphere with the exhaust gases in vehicles with ICE was stored with the help of nanoparticles ($Al_2O_3$) addition PCM. The cabin interior heating process of a typical sedan automobile in cold climate conditions is used as the heat discharge medium for the LHTES system. In experiments performed under real climatic conditions for 1200 sec (i.e., 20 min), the effects on the cabin interior heating and solidification processes were investigated of the pure paraffin (RT55) and 5 different nanoparticles ($Al_2O_3$) fractions (5 wt.%, 10 wt.%, 15 wt.%, 20 wt.%, and 25 wt.%). The results obtained showed that higher cabin interior heating performance and an improved solidification process were obtained with a 10 wt.% $Al_2O_3$ addition to RT55.

## 2. Material and Method

The main setup of this paper covers the use of exhaust waste heat energy stored in the PCM container of a typical automobile travelling in cold climate conditions for the heating of the automobile cabin under the next first cold start conditions (i.e., one night or a few hours later). In addition, the effect of the $Al_2O_3$ nanoparticle addition in PCM on the capability of the interior cabin heating system was also investigated. In this paper, Rubitherm RT55 was used as the PCM material. The cabin interior of a typical sedan automobile was used as the heat discharge medium for the solidification process of the RT55. The thermophysical properties of RT55 is given in Table1.

Table 1. Thermophysical properties of RT55 [27]

| Density (kg/m$^3$) | 880/770 |
|---|---|
| Melting area (°C) | 51-57 (mean peak = 55) |
| Congealing area (°C) | 56-57 |
| Specific heat (cp) – (kj/kgK) | 2 |
| Thermal conductivity (W/mK) | 0.2 |
| Latent heat of fusion (kJ/kg) | 170 |
| Volume expansion (%) | 14 |
| Flashpoint (°C) | >200 |
| Max. operation temperature (°C) | 90 |

The tank in which RT55 is stored is designed to be two-layered and cylindrical and produced from optical (plexiglass) material. The inner shell of the latent heat storage tank has an outer diameter of 280 mm, a height of 350 mm, and a wall thickness of 10 mm; the outer shell was designed to have an outer diameter of 350 mm, a height of 350 mm, and a wall thickness of 5 mm and was supplied on the market. In this way, the solidification process of RT55 was visualized during the experiments. Heat insulation is provided by applying vacuum pressure between the inner and outer layers of the tank. The upper and lower covers of the latent heat storage container are also made of PMMA material, so the melting process of the PCM is fully visualized. The bottom cover has a diameter of 280 mm and a height of 10 mm. The top cover has a diameter of 280 mm and a height of 20 mm. To realize the heat transfer from the tank where the PCM is stored to the working fluid, a coil type heat exchanger consisting of 3 layers inside each other made of copper pipes was used. The coil type heat exchanger is named the middle, first, and second coil. It is designed and manufactured with a distance of 375 mm between each coil. The middle coil has a height of 160 mm and an outer diameter of 15 mm, is produced with a wall thickness of 1 mm, and is positioned in the center of the PCM heat exchanger. The first and second coils are produced in helical geometry. The first coil helix diameter is 90 mm, the helix height is 160 mm, and the number of helices is 8. The helix diameter of the second coil is 194 mm, with a 160 mm helix diameter and 8 helices. Copper pipes with an outer diameter of 10 mm and a thickness of 1 mm were used for the production of the first and second coils. Copper welding was used to connect the three copper pipes produced. The coil type heat exchanger consisting of 3 layers is given in Fig.1.



Fig.1. Coil type heat exchanger consisting of 3 layers

For the purpose of heating the cabin, the heater radiator of a typical sedan car is placed in the rear seat compartment of the automobile in a position to blow hot air into the cabin interior. A closed-circuit liquid circulation system is used between the copper coil heat exchangers in the PCM tank and the central heating radiator in the cabin of the automobile. A mixture of 75% ethylene glycol and 25% tap water by volume was used as the heat transfer fluid (HTF). The HTF is circulated at a 3 l/d mass flow rate in the closed-circuit fluid circulation system by using a 12 V DC electrically powered water pump. A liquid/steam separator is added to prevent the possible formation of steam in the closed-loop liquid circulation system. As fasteners in the experimental setup, rubber water pipes with fabric braided resistant to temperature are used. A one-way air valve and a vacuum pump are used to provide the vacuum environment in which heat insulation is created between the shells. During the experiments, the temperature of the RT55 in

the PCM container, the surface temperature of the PCM tank, the inlet and outlet temperature of the HTF, the temperature of the air at the heating radiator outlet, and the automobile cabin interior temperature were measured. The schematic picture of the experimental setup is given in Fig.2.
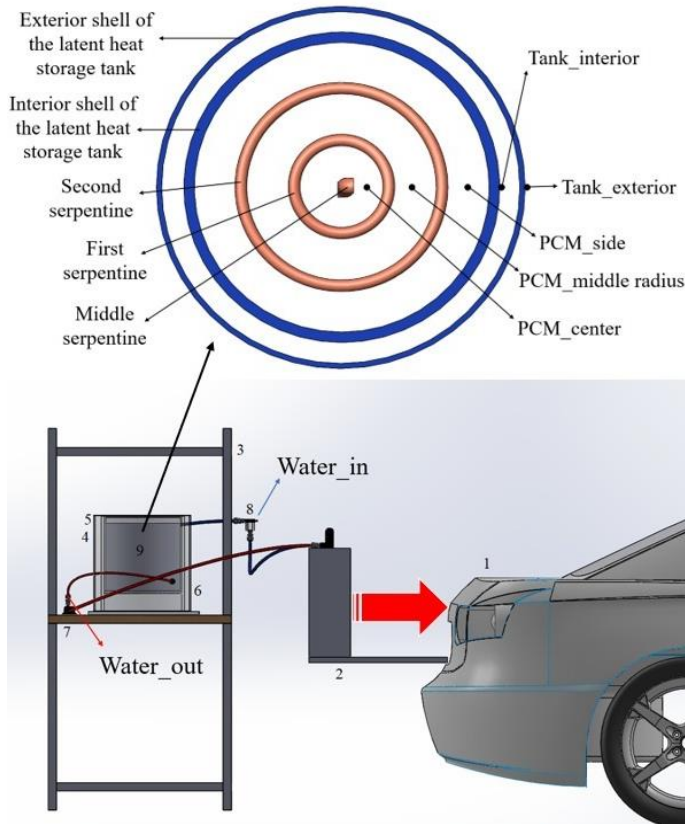


1. Interior of automobile, 2. Radiator in automobile cabin, 3. Test bench, 4. PCM heat exchanger, 5. Upper plate, 6. Middle plate 7. DC water pump, 8. Liquid/vapor separator, 9. RT-55 paraffin wax

Fig.2. Schematic picture of the experimental setup

Experimental studies were carried out under real-world climatic conditions (2 °C) for 20 minutes. Experimental studies were repeated for pure paraffin wax and 5 different nanoparticles (Al2O3) addition fractions (5 wt.%, 10 wt.%, 15 wt.%, 20 wt.%, and 25 wt.%).

## 3. Results and Discussion

The time-dependent variation of air temperature at the fan outlet for different $Al_2O_3$ fractions is given in Fig.3. In the heat discharge (solidification) process initiated at 2 °C ambient temperature conditions, the air temperature at the fan outlet for the pure paraffin ve $Al_2O_3$ fractions (5 wt.%, 10 wt.%, 15 wt.%, 20 wt.%, and 25 wt.%) has reached 9.9 °C, 13.1 °C, 13.8 °C, 12.6 °C, 11.6 °C, and 10.8 °C after 1200 sec, respectively. It is seen that the air temperature at the fan outlet increases up to 10 wt.% $Al_2O_3$ fractions, and more $Al_2O_3$ addition causes a decrease in the temperature at the fan outlet. So much so that, with 25 wt.% $Al_2O_3$ fractions, the temperature at the fan outlet is quite close to pure RT55. At 1200 seconds, the increase in fan outlet

temperature for 5 wt.% $Al_2O_3$ and 10 wt.% $Al_2O_3$ fractions compared to pure paraffin (RT55) is 32.3% and 39.4%, respectively. It should be noted that the rate of increase is quite high up to 5 wt.%, and the rate of increase is considerably slowed by increasing the $Al_2O_3$ fraction to 10 wt.%. However, with 10 wt.% $Al_2O_3$ fractions, it is clear that the fan outlet temperature throughout the entire experiment was considerably higher than both pure RT55 and other $Al_2O_3$ fractions. On the other hand, it is seen that the air temperature increase rate at the fan outlet slows down considerably after 600th seconds in the 10 wt.% $Al_2O_3$ fractions. The main reason for this is the thermal conductivity variation of $Al_2O_3$ nanoparticles added to PCM with temperature. With the increase in operating temperature, the tendency of TC first increases, then decreases, and finally again gradually increases [28]. On the other hand, the heat capacity of nanoparticle-enhanced composite PCMs at high temperatures (liquid phase) is greater than at low temperatures (solid phase) [29].
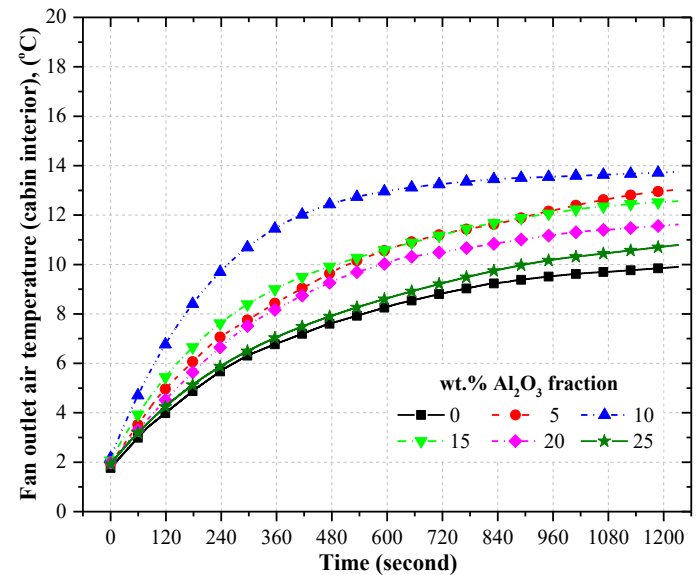


Fig.3. Time-dependent variation of air temperature at the fan outlet for different $Al_2O_3$ fractions

The time-dependent variation of the cabin interior air temperature of an automobile for different $Al_2O_3$ fractions is given in Fig.4. In the in-cabin heating process, initiated at 2 °C ambient temperature conditions, at 1200th sec, the cabin interior air temperature of the automobile for the pure paraffin wax (RT55) ve $Al_2O_3$ fractions (5 wt.%, 10 wt.%, 15 wt.%, 20 wt.%, and 25 wt.%) has reached 6.2 °C, 7.7 °C, 8.0 °C, 7.3 °C, 6.8 °C, and 6.5 °C, respectively. The cabin interior temperature increased up to 10 wt.% $Al_2O_3$ fraction compared to pure RT55, and started to decrease again with the further increase of the $Al_2O_3$ fraction. The main reason is that the $Al_2O_3$ nanoparticles improve the heat transfer coefficient and thermal stability of pure paraffin [30]. Because the nanoparticles dispersed in PCM contribute to the improvement of the melting and solidification processes by increasing the thermal conductivity due to its high surface area-to-volume ratio [31]. In addition, $Al_2O_3$ nanoparticles have higher thermal conductivity than PCM. Therefore, the thermal conductivity increases with an increasing $Al_2O_3$ nanoparticle

fraction [32]. On the other hand, the addition of nanoparticles to PCM causes a reduction in the sensible heat stored in the melting/solidification process, resulting in a decrease in the specific heat capacity. Therefore, a decrease in the heat of fusion occurs during the charge and discharge process of the nanoparticle added PCM compared with the pure PCM [33]. As a result, the addition of 10% more $Al_2O_3$ nanoparticles had a negative effect on the solidification process as it reduced the heat of fusion too much. Therefore, the cabin interior temperature has also decreased due to the reduction in the rate of heat transfer from the high-temperature RT55 with more than 10 wt.% $Al_2O_3$ fraction to the HTF circulated in the cabin interior. At 1200 seconds, the increase in the cabin interior temperature for 5 wt.% $Al_2O_3$ and 10 wt.% $Al_2O_3$ fractions compared to pure RT55 is 24.2% and 29%, respectively. While the temperature increase in the cabin is quite high, up to 5 wt.% by weight of $Al_2O_3$ fraction, the temperature increase is slower by 10 wt.% of $Al_2O_3$ fraction. On the other hand, it is worth mentioning that other $Al_2O_3$ fractions (i.e., 15 wt.%, 20 wt.%, and 25 wt.%) also have higher cabin interior air temperatures compared to RT55 at 1200th sec. Compared to pure paraffin, the increase in cabin interior air temperature with 15 wt.%, 20 wt.%, and 25 wt.% $Al_2O_3$ fractions is 17.7%, 9.7%, and 4.8%, respectively. As can be seen, when the $Al_2O_3$ fraction is increased by more than 10 wt.%, the cabin interior temperature decreases again and approaches pure RT55.
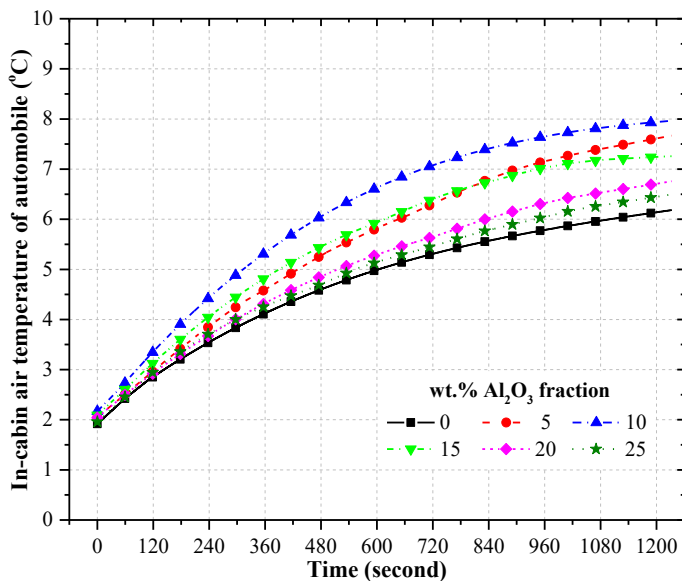


Fig.4. Time-dependent variation of the cabin interior air temperature of the automobile for different $Al_2O_3$ fractions

The time-dependent variation of PCM temperature for different $Al_2O_3$ fractions is given in Fig.5. The PCM temperature is approximately 93 °C at the beginning of all experiments. At end of the experiments, the PCM temperature for the pure RT55) ve $Al_2O_3$ fractions (5 wt.%, 10 wt.%, 15 wt.%, 20 wt.%, and 25 wt.%) has reduced at 76.3 °C, 66.9 °C, 65.7 °C, 68.5 °C, 70.1 °C, and 72.2 °C, respectively. It should be noted that a lower PCM temperature at 1200 th seconds is indicative of a more advanced

solidification process. Because the lower temperature in the heat discharge process is an indication that more mass in the PCM tank is participating and/or completing in the solidification process, as an indicator of the liquid phase to solid phase conversion of the RT55. However, PCM temperature, which decreased until 10 wt.% $Al_2O_3$ nanoparticles fraction, started to increase again. The main reason for this is that although the thermal conductivity of $Al_2O_3$ nanoparticles added to the PCM increases, the latent heat capacity decreases. Mishra et al. state that more than 5% nanoparticle addition to PCM reduces the thermal energy storage capacity, so the nanoparticle fraction should be added at a rate that provides an efficient phase change process and optimum energy storage capacity [34]. On the other hand, Mehdi and Nsofor tried nanoparticle volume fractions in the range of 0–8% in FDM and achieved the highest improvement with the addition of 8 vol.% $Al_2O_3$ nanoparticles for the solidification process [35]. At 1200 th seconds, the decreases in PCM temperature for 5 wt.% $Al_2O_3$, 10 wt.% $Al_2O_3$, 15 wt.% $Al_2O_3$, 20 wt.% $Al_2O_3$, 25 wt.% $Al_2O_3$ fractions compared to pure RT55 are 14.1%, 16.1%, 11.4%, 8.8%, and 5.7%, respectively. An important result to note is that the decrease in PCM temperature slows down considerably after the 720th second, especially at the 10 wt.% $Al_2O_3$ fractions.
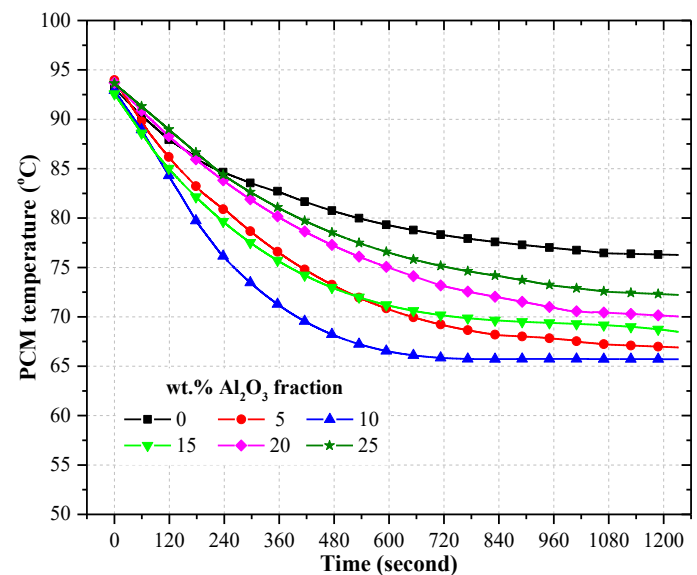


Fig. 5. Time-dependent variation of PCM temperature for different $Al_2O_3$ fractions

The time-dependent variation of HTF inlet and outlet temperatures for different $Al_2O_3$ fractions is given in Fig.6. At the beginning of the experiments, for pure RT55 and $Al_2O_3$ fractions, the HTF inlet temperature changed in the range of 13–17 °C depending on the ambient and experimental operating conditions, and the HTF outlet temperature changed in the range of 35–40 °C. In general, the difference (between 0.72–0.96 °C) between HTF inlet and outlet temperatures decreased considerably at the end of the experiments (at 1200th sec.) for both pure RT55 and $Al_2O_3$ fractions compared with the beginning of the experiments. The main reason for this expected result is the decrease in the heat transfer rate to the HTF due to the decrease in RT55

279

temperature with the solidification process. In addition, the fact that the difference between the HTF inlet and outlet temperature is very close to each other indicates that the amount of heat energy to be transferred from the RT55 to the HTF is now very limited. In Fig.6, the rapid increase in water inlet and outlet temperatures up to 240th sec. under the conditions of 10 wt.% $Al_2O_3$ fractions is remarkable. This finding is a result of the increase in heat transfer rate from RT55 to HTF with 10 wt.% $Al_2O_3$ fractions and resulted in an increase in cabin interior temperature where HTF is circulated, as shown in Fig.4. As expected, as a result of increasing the $Al_2O_3$ fraction added to the PCM, the heat transfer rate was increased and the phase change process accelerated [36]. Abdulateef et al. mentioned that the addition of 10% $Al_2O_3$ increased the thermal conductivity of PCM by 25%. So much so that adding 10% $Al_2O_3$ nanoparticles by volume can increase pure paraffin's thermal conductivity from 0.2 W/mK to 0.265 W/mK [37]. On the other hand, the addition of $Al_2O_3$ increased by (10 wt.%) more than enough to decrease, more than can be tolerated, the heat storage capacity of the nanoparticle-enhanced composite PCM. So much so, with the addition of 5 vol.% $Al_2O_3$ nanoparticles compared to pure paraffin, the total enthalpy can decrease by approximately 10.9% [38]. In addition, throughout the experiment, the HTF inlet and outlet temperature increase of pure RT55 is low. While the HTF inlet and outlet temperature rates increased up to 10 wt.% $Al_2O_3$ fractions, the HTF inlet and outlet temperature increase rates slowed down again when the $Al_2O_3$ fraction increased further. So much so that under the conditions of 25 wt.% $Al_2O_3$ fraction, the HTF inlet and outlet temperatures remained almost constant after 360th sec.

ments, depending on the temperature of the RT55 in the container, the surface temperature of the inner shell changed between 63.6 °C and 71 °C, and the surface temperature of the inner shell changed between 34 °C and 37.5°C. However, it is seen that the lowest inner and outer shell surface temperatures are obtained with 10 wt. % $Al_2O_3$ fractions. Despite the high rate of decrease in the inner shell surface temperature for all experimental conditions, the outer shell surface temperature decreases very slowly. This result is proof that an effective thermal insulation is provided in the PCM tank with the vacuum pressure applied between the inner and outer shell.
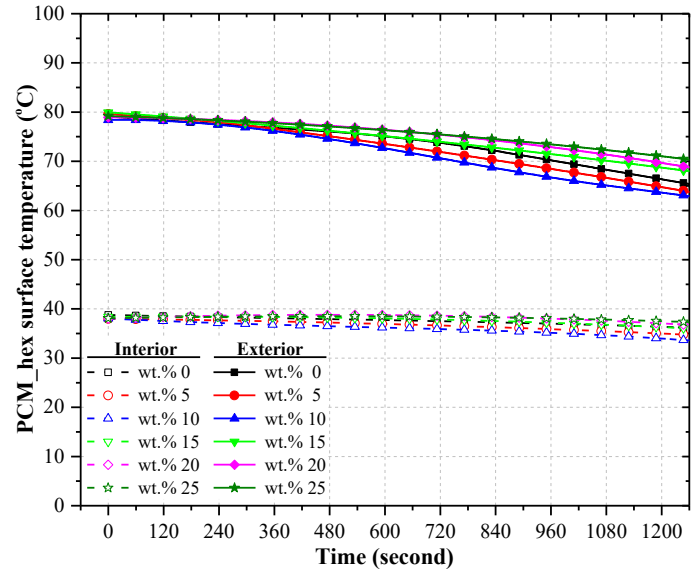


Fig. 7. Time-dependent variation of the inner and outer shell surface temperatures for different $Al_2O_3$ fractions

Fig.8 shows the solidification images of pure RT55 and 5 wt.%, 10 wt.%, 15 wt.%, 20 wt.%, and 25 wt.% of $Al_2O_3$ fractions at 1200th sec. First, the solidification process is evident to proceed from the bottom of the PCM vessel to the top cover for all experimental conditions. As seen in Fig.8, with the addition of $Al_2O_3$ into pure paraffin RT55, the solidification process improved at the end of the 1200th second and the amount of RT55 solidified in the PCM tank increased. It is seen that the solidification process increases considerably in the PCM tank where the 10 wt.% $Al_2O_3$ fraction is provided, and the solidification reaches as far as the outer walls of the vessel and the coil type heat exchangers become invisible. However, in pure RT55 conditions, the solidification process appears to be limited to the coil type heat exchanger surfaces. It is seen that there are improvements in the solidification process with the other $Al_2O_3$ fractions (5 wt.%, 15 wt.%, 20 wt.%, and 25 wt.%). However, it is clearly seen that the optimum $Al_2O_3$ fraction is 10 wt.%. Literature studies visualizing the phase change process show that the positive effect of the addition of $Al_2O_3$ on the melting and solidification process of PCM is greater than the fins placed around the heat transfer tube. In addition, numerical model studies show that the addition of $Al_2O_3$ to PCM affects the solidification process more than the melting process. For example, for the same PCM_hex design, melting and solidification times



Fig 6. Time-dependent variation of HTF inlet and outlet temperatures for different $Al_2O_3$ fractions

The time-dependent variation of inner and outer shell surface temperatures for different $Al_2O_3$ fractions is given in Fig.7. The inner and outer shell surface temperatures for pure RT55 and $Al_2O_3$ fractions were approximately 38 °C and 80 °C, respectively, at the start of the experiments. At the end of the experi-

were decreased by 6.4% and 12%, respectively, with the addition of 5% $Al_2O_3$ [39]. In contrast, the result of another experimental study shows that the addition of 5% $Al_2O_3$ nanoparticles reduces the melting process 3.5 times and the solidification process 2.25 times [33]. Singh et al. obtained a 22.6% improvement in the solidification time compared to pure paraffin with the addition of a 0.5% volume concentration of $Al_2O_3$ nanoparticles into PCM [38].



| Pure RT55 paraffin wax | 5 wt.% $Al_2O_3$ | 10wt. % $Al_2O_3$ |
| 15 wt. %$Al_2O_3$ | 20 wt.% $Al_2O_3$ | 25 wt.% $Al_2O_3$ |
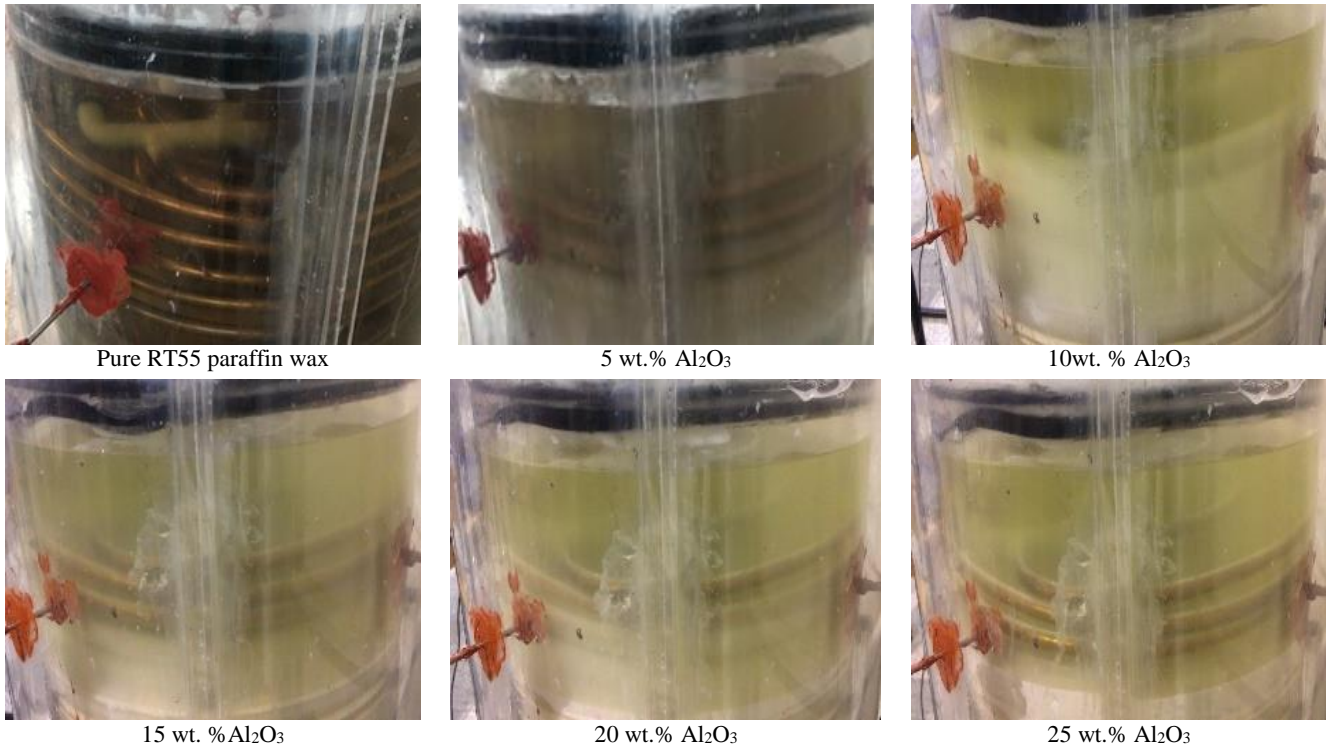
Fig. 8. Pure RT55 and 5 wt.%, 10 wt.%, 15 wt.%, 20 wt.% and 25 wt.% solidification images of $Al_2O_3$ fractions at 1200th second

## 4. Conclusions

The results of this study, in which the ICE vehicle exhaust waste heat energy is stored in the LHTES system using nanoparticles ($Al_2O_3$) added to PCM, and is used for cabin interior heating in cold climate conditions (2 °C), are summarized as follows:

- The addition of up to 10 wt.% $Al_2O_3$ to pure paraffin improved the solidification process and raised the cabin interior temperature. The increases in the cabin interior temperature for 5 wt.% $Al_2O_3$ and 10 wt.% $Al_2O_3$ fractions compared to pure RT55 are 24.2% and 29%, respectively.
- The addition of more than 10 wt.% $Al_2O_3$ to RT55 resulted in a worsening of the solidification process and a cabin interior temperature decrease. However, higher solidification performance and, therefore, cabin interior temperature is obtained with all $Al_2O_3$ fractions compared to pure RT55. According to pure RT55, the increase in cabin interior temperature with 15 wt.%, 20 wt.%, and 25 wt.% $Al_2O_3$ fractions is 17.7%, 9.7%, and 4.8%, respectively.
- At the end of the heat discharge process initiated at 2 °C ambient temperature (during 1200 sec.), cabin interior temperatures for the pure paraffin and $Al_2O_3$ fractions (5 wt.%, 10 wt.%, 15 wt.%, 20 wt.%, and 25 wt.%) arrived at 6.2 °C, 7.7 °C, 8.0 °C, 7.3 °C, 6.8 °C, and 6.5 °C, respectively.
- With the vacuum pressure applied to the cylindrical space formed between the inner and outer shell of the PCM container, which is made of 2-layer optical material, an effective heat insulation was achieved under all experimental conditions.
- In future waste heat recovery studies to be carried out with nanoparticle added PCM, it is important to examine the effect of the addition of nanoparticle additives (i.e., CuO, CuO-MWCNT) other than $Al_2O_3$ into both PCM and HTF on the melting and solidification process. In addition, in order to optimise the $Al_2O_3$ fraction, the range of 5–10% should be examined by 1 wt.% $Al_2O_3$ fraction increments.

## Credit of Interest Statement

The authors declare that there is no conflict of interest in the paper.

## CRediT Author Statement

**Habib Gürbüz:** Supervision, Investigation, Conceptualization, Methodology, Writing - review & editing, Visualization

**Himmet Emre Aytaç:** Experimental setup, Data collection, Writing-original draft, Visualization

**Hüseyin Cahit Hamamcıoğlu:** Experimental setup, Data collection, Writing-original draft, Visualization

**Hüsameddin Akçay:** Experimental setup, Data collection, Writing-original draft, Visualization

## References

[1] Jadhao JS, Thombare, DG. Review on Exhaust Gas Heat Recovery for IC Engine. Int J Eng Innov 2013;2(2):93-100.

[2] Endo T, Kawajiri S, Kojima Y, Takahashi K, Baba T, Ibaraki S, Shinohara M. Study on maximizing exergy in automotive engines. SAE trans 2007;347-356.

[3] Teng H, Regner G, Cowland C. Waste heat recovery of heavy-duty diesel engines by organic Rankine cycle Part II: working fluids for WHR-ORC. SAE trans 2007;01:0543.

[4] Mollenhauer E, Christidis A, Tsatsaronis G. Increasing the Flexibility of Combined Heat and Power Plants with Heat Pumps and Thermal Energy Storage. J Energy Resour Technol 2018;140(2):020907.

[5] Gürbüz H, Ateş D. A numerical study on processes of charge and discharge of latent heat energy storage system using RT27 paraffin wax for exhaust waste heat recovery in a SI engine. Int J Automot Technol 2020;4 (4):314-327.

[6] Karasu H, Dincer I. Analysis and Efficiency Assessment of Direct Conversion of Wind Energy into Heat Using Electromagnetic Induction and Thermal Energy Storage, J Energy Resour Technol 2018;140(7):071201.

[7] Dincer I, Rosen MA. Thermal energy storage (TES) methods. Thermal Energy Storage: Systems and Applications. New York: John Wiley & Sons. 2002;93–212.

[8] Huggins RA. Energy storage, Fundamentals: Materials and Applications. Springer-Verlag GmbH; 2010.

[9] Nazir H, Batool M, Osorio FJB, Isaza-Ruiz M, Xu X, Vignarooban K, Phelan P, Inamuddin, Kannan AM. Recent developments in phase change materials for energy storage applications: A review. Int J Heat Mass Transf 2019;129:491-523.

[10] Raoux S, Welnic W, Ielmini D. Phase change materials and their application to nonvolatile memories. Chem Rev 2010;110:240-267.

[11] Swathykrishnan B, Sreelakshmi C, Duggal P, Tomar RK. Application of Phase Change Materials in Buildings. In 2020 International Conference on Intelligent Engineering and Management (ICIEM), 2020;203-206.

[12] Kumar N, Banerjee D. Phase Change Materials. Handbook of Thermal Science and Engineering, Springer 2018;2213-2275.

[13] Jaguemont J, Omar N, Van den Bossche P, Mierlo J. Phase-change materials (PCM) for automotive applications: A review. Appl Therm Eng 2018;132:308-320.

[14] Rathod MK. Phase Change Materials and Their Applications. Phase Change Materials and Their Applications, 2018;37-57.

[15] Sharma A, Tyagi VV, Chen CR, Buddhi D. Review on thermal energy storage with phase change materials and applications. Renew Sust Energ Rev 2009;3(2):318-345.

[16] Rathod MK. Phase Change Materials and Their Applications. Phase Change Materials and Their Applications, London 2018;3:37-57.

[17] Dhinakaran R, Muraliraja R, Elansezhian R, Baskar S, Satish S, Shaisundaram VS. Utilization of solar resource using phase change material assisted solar water heater and the influence of nano filler. Materials Today: Proceedings 2021;37:1281-1285.

[18] Kumar PM, Sudarvizhi D, Stalin PMJ, Aarif A, Abhinandhana R, Renuprasanth A, Ezhilan NT. Thermal characteristics analysis of a phase change material under the influence of nanoparticles. Materials Today: Proceedings 2021;45:7876-7880.

[19] Elbahjaoui R, El Qarnia H. Performance evaluation of a solar thermal energy storage system using nanoparticle-enhanced phase change material. Int J Hydrog Energy 2019;44(3):2013-2028.

[20] Aqib M, Hussain A, Ali HM, Naseer A, Jamil F. Experimental case studies of the effect of $Al_2O_3$ and MWCNTs nanoparticles on heating and cooling of PCM. Case Stud Therm Eng 2020;22:100753.

[21] Haghighi A, Babapoor A, Azizi M, Javanshir Z, Ghasemzade H. Optimization of the thermal performance of PCM nanocomposites. JEMT 2020;4(2):14-19.

[22] Mahdi JM, Nsofor EC. Solidification enhancement of PCM in a triplex-tube thermal energy storage system with nanoparticles and fins. Appl Energy 2018;211:975-986.

[23] Wu SY, Wang H, Xiao S, Zhu DS. An investigation of melting/freezing characteristics of nanoparticle-enhanced phase change materials. J Therm Anal Calorim 2012;110(3): 1127-1131.

[24] Darzi AAR, Jourabian M, Farhadi M. Melting and solidification of PCM enhanced by radial conductive fins and nanoparticles in cylindrical annulus. Energy Convers Manag 2016; 118:253-263.

[25] Motahar S, Alemrajabi AA, Khodabandeh R. Experimental study on solidification process of a phase change material containing $TiO_2$ nanoparticles for thermal energy storage. Energy Convers Manag 2017;138:162-170.

[26] Gürbüz H, Ateş D. An investigation of the melting process in a latent heat thermal energy storage system using exhaust gases of a spark ignition engine. Proc Inst Mech Eng D: J Automob Eng 2022;1-16.

[27] Rubitherm, PCM RT-Line. https://www.rubitherm.eu/en/index.php/productcategory/organische-pcm-rt, 2022 (Access: 5 January 2022).

[28] Li D, Wang Z, Wu Y, Liu C, Arıcı M. Experimental investigation on thermal properties of $Al_2O_3$ nanoparticles dispersed paraffin for thermal energy storage applications. Energy Sources A: Recovery Util Environ Eff 2021;0(0):1-11.

[29] Babapoora A, Karimia G, Sabbaghi S. Thermal characteristic of nanocomposite phase change materials during solidification process. J Energy Storage 2016; 7:74–81.

[30] Bahari M, Najafi B, Babapoor A. Evaluation of α-AL2O3-PW nanocomposites for thermal energy storage in the agro-products solar dryer. J Energy Storage 2020; 28:101-181.

[31] Sarbu I, Sebarchievici C, A comprehensive review of thermal energy storage, Sustainability 2018;10(1):191.

[32] Mohammadi O, Shafii MB, Rezaee Shirin-Abadi A, Heydarian R, Ahmadi MH. The impacts of utilizing nanoencapsulated PCM along with RGO nanosheets in a pulsating heat pipe, a comparative study. Int J Energy Res. 2021; 45:19481–19499.

[33] Gunjo DG, Jena SR, Mahanta Pi, Robi PS. Melting enhancement of a latent heat storage with dispersed Cu, CuO and $Al_2O_3$ nanoparticles for solar thermal application. Renew 2018; 121:652-665.

[34] Mishra DK, Bhowmik S, Pandey KM. Analysis of Heat Transfer Rate for Different Annulus Shape Properties-Enhanced Beeswax-Based Phase Change Material for Thermal Energy Storage. Math Probl Eng 2020; 6123472:21.

[35] Mahdi JM, Nsofor EC. Solidification enhancement of PCM in a triplex-tube thermal energy storage system with nanoparticles and fins. Appl. Energy 2018; 211:975-986.

[36] Saeed AM, Abderrahmane A, Qasem NAA, Mourad A, Alhazmi M, Ahmed SE, Guedri K. A numerical investigation of a heat transfer augmentation finned pear-shaped thermal energy storage system with nano-enhanced phase change materials. J Energy Storage 2022; 53:105172.

[37] Abdulateef AM, Jaszczur M, Hassan Q, Anish R, Niyas H, Sopian K, Abdulateef J. Enhancing the melting of phase change material using a fins–nanoparticle combination in a triplex tube heat exchanger, J

Energy Storage 2021;35:102227.

[38] Singh SK, Verma SK, Kumar R. Thermal performance and behavior analysis of $SiO_2$, $Al_2O_3$ and MgO based nano-enhanced phase-changing materials, latent heat thermal energy storage system. J Energy Storage 2022; 48:103977.

[39] Keshteli AN, Sheikholeslami M. Influence of $Al_2O_3$ nanoparticle and Y-shaped fins on melting and solidification of paraffin. J Mol Liq 2020; 314:113798.